Multifunctional dual-tunable low loss ferrite-ferroelctric heterostructures for microwave devices

Jaydip Das[a)]
Department of Physics, Colorado State University, Fort Collins, Colorado 80523, USA

Boris A. Kalinikos
Department of Physics, Colorado State University, Fort Collins, Colorado 80523, USA and St. Petersburg Electrotechnical University, 197376 St. Petersburg, Russia

Arkajit Roy Barman and Carl E. Patton
Department of Physics, Colorado State University, Fort Collins, Colorado 80523, USA

(Received 10 September 2007; accepted 4 October 2007; published online 25 October 2007)

Oriented barium ferrite (BaM) and polycrystalline ferroelectric barium strontium titanate (BSTO) layered structures have been fabricated by pulsed laser deposition. The 0.5 μm thick BaM layer has a saturation induction of 4 kG, a uniaxial effective anisotropy field of 16 kOe, and a relatively low ferromagnetic resonance linewidth of about 25 Oe, values that are indicative of a high quality film. The dielectric constant of the 0.9 μm thick BSTO layer drops by a factor of 2 for an applied voltage of 3 V. © *2007 American Institute of Physics*. [DOI: 10.1063/1.2802577]

The physical properties of ferrite-ferroelectric heterostructures and composites have been a subject of intense recent interest due to the unique possibility of dual magnetic and electric field tunability.[1–3] The magnetic field tunable ferrite materials, on the one hand, are widely utilized for microwave and millimeter wave applications. In suitable devices, bulk and thin film ferrite materials can yield high figures of merit, wide bandwidths, low insertion loss, and frequency agility. Current bulk ferrite components, however, also present several critical problems for advanced applications. These include the large size and weight for the required electromagnets, the lack of fast tunability, and the lack of planar integratibility. Ferroelectric materials, on the other hand, have electric field tunablility[4] that can be achieved through the application of a modest voltage with a negligible current drain. Even though the electric frequency tunability is not generally as wide as magnetic field tuning in ferrite devices, it is usually faster and imposes a much smaller and essentially negligible power consumptions.

Ferrite-ferroelectric materials in a layered or composite structure provide the possibility of simultaneous broadband magnetic field and fast electric field tuning. This can give rise to fast, cost effective, small size planar, and broadband devices for a wide range of high frequency applications. Attempts have been made to fabricate such structures with yttrium iron garnet and barium strontium titanate (BSTO) and simultaneous, albeit narrow band, tunability has been demonstrated for frequencies up to 5 GHz or so.[5,6] However, there has been a limited attempt to extend these capabilities to include wide band electric field tuning and millimeter wave band frequencies.[7]

The proper choice of a high anisotropy ferrite component is critical to millimeter wave applications. Hexagonal barium ferrite (BaM) materials in general and thin films in particular, with a large effective uniaxial anisotropy field of about 17 kOe, can be tuned to ferromagnetic resonance (FMR) at frequencies of 40–50 GHz and higher with relatively small applied magnetic fields. Recent advances in the growth of BaM films with low microwave loss at high frequency make these materials extremely attractive for such applications. The case is made even stronger by recent work to grow thick films and films with in-plane *c*-axis and in-plane uniaxial anisotropy directions.[8]

These advances in techniques for the fabrication of BaM films raise the possibility of hexagonal ferrite film based ferrite-ferroelectric layered structures for dual tunability wide band millimeter wave devices. Films with alternating layers of BaM and BSTO and related ferroelectric materials, for example, with embedded electrodes for electric field tuning, may offer an ideal way to realize such devices. This paper reports on the realization of such structures that combine a high quality low loss BaM layer, a BSTO layer with a reasonable dielectric tunability, and functional electrodes for the electric field tuning.

The BaM/electrode/BSTO/electrode structures were grown on *c*-cut sapphire by pulsed laser deposition (PLD) for the ferrite and ferroelectric layers and sputtering for the gold electrodes. Combined scanning electron microscopy (SEM) and energy dispersive spectroscopy (EDS) measurements, along with x-ray diffraction (XRD), were used for characterization. Hysteresis loop and FMR measurements were used for magnetic characterizations. Capacitance measurements were used to study the dielectric properties and electric tunability of the BSTO component. The data show that the separate ferrite and ferroelectric component layers do not degrade appreciably in the layered structure. The SEM and XRD results show the presence of distinct layers of *c*-axis oriented BaM and polycrystalline BSTO. The hysteresis loop and FMR results show the clear uniaxial and low loss properties of the BaM. The capacitance measurements show a substantial electric field tunability of the BSTO.

The BaM component was first deposited on the sapphire substrate by PLD methods with a Lambda Physik 248 nm KrF laser and a commercial polycrystalline BaM target. The proper choice of all deposition parameters play a critical role in the realization of quality films.[9,10] For these structures, the deposition was done at a laser fluence and pulse repetition

[a)]Electronic mail: jaydip@lamar.colostate.edu

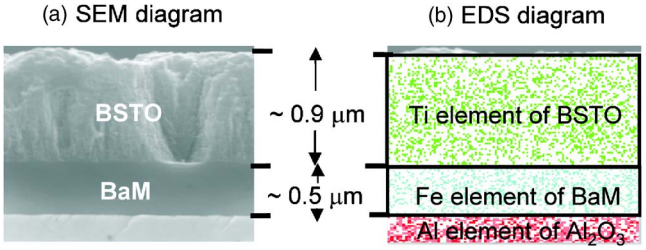

FIG. 1. (Color online) (a) SEM of the 0.5 μm thick BaM and the 0.9 μm thick BSTO layered structure. (b) Element specific EDS results for the same film.

rate of 1.3 J/cm^2 and 25 Hz, respectively, onto a 910 °C substrate positioned 5.5 cm from the target, in a 600 mTorr pure oxygen atmosphere, and for a deposition time of 20 min. Slow cooling was done *in situ*, with the oxygen pressure increased to 400 Torr. The films were then removed from the PLD system and annealed at 1050 °C in flowing oxygen. The annealing step is critical for stress reduction and the realization of films with low microwave loss. The nominal BaM film thickness was about 0.5 μm. The embedded 30 nm gold electrode layer was then sputter deposited on the annealed BaM film.

The polycrystalline BSTO layer was deposited in the same PLD system. A commercial polycrystalline $Ba_{0.5}Sr_{0.5}TiO_3$ target was used. The substrate temperature was set at 600 °C. The laser fluence and oxygen pressure were kept the same as for the BaM, but the target-substrate distance increased to 6.5 cm to accommodate for the larger plume. Film thicknesses of 0.9 μm were then realized with a laser pulse repetition rate and deposition time of 15 Hz and 26 min, respectively. A 50 nm gold capping electrode was sputter deposited to complete the structure.

The (a) and (b) images in Fig. 1 show representative SEM and EDS results, respectively, for the BaM-BSTO structure. The red, blue, and green regions in (b) show the aluminum, iron, and titanium element EDS traces for the sapphire substrate, the BaM layer, and the BSTO layer, respectively. If one zooms in on different points in the cross section shown and performs local EDS composition analyses, one obtains atomic percentages that closely match those expected for BSTO and BaM.

Figure 2 shows XRD results. Graph (a) shows the XRD pattern with the sample oriented to maximize the peaks from the sapphire substrate. This also serves to bring out the maximum signal from the BaM layer. Graph (b) shows the corresponding pattern with the sample oriented to minimize the substrate peaks. This serves to bring out the BSTO signal. From (a), one can see distinct peaks for the *c*-axis oriented BaM layer. Upon close examination, one can also identify weak BSTO (110) and (111) peaks on the right shoulders of BaM (0008) and (00010) peaks, respectively. The differences in intensities are due to the fact that the BaM layer is epitaxial and the BSTO layer is comprised of randomly oriented polycrystalline grains. From (b), one sees well-resolved peaks that may be associated with polycrystalline BSTO. These data also show peaks associated with the oriented BaM as well as a weak gold peak. It is the oriented nature of the BaM and sapphire components that allows one to use an in-plane rotation to deemphasize these signals and bring out the polycrystalline BSTO signal.

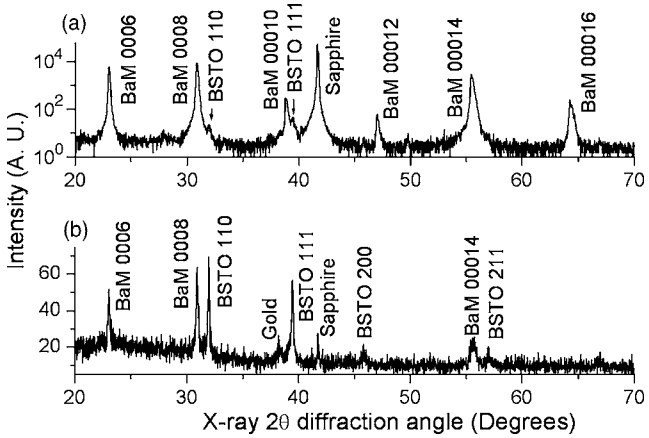

FIG. 2. X-ray diffraction patterns of the BaM-BSTO structure as a function of the x-ray 2θ diffraction angle. Graphs (a) and (b) show data for film orientations that maximize and minimize the substrate signal, respectively. The labels identify various peaks in the spectra.

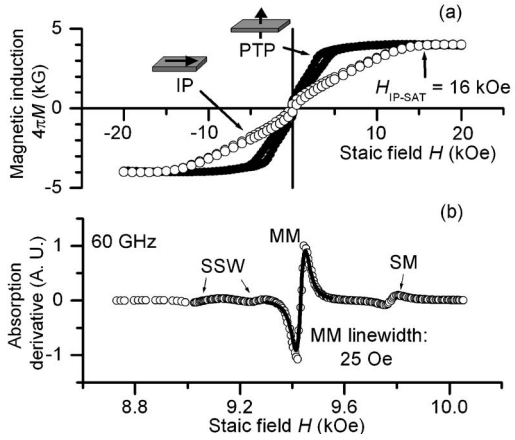

FIG. 3. (a) Induction $4\pi M$ vs static field H for PTP and IP fields with the IP saturation field $H_{IP\text{-}sat} \approx 16$ kOe, as indicated. (b) 60 GHz ferromagnetic resonance absorption derivative vs H profile. Labels designate the main mode (MM), the low field standing spin wave (SSW) modes, and the high field surface mode (SM). The solid line shows a Lorentzian derivative best fit to the MM data. The narrow linewidth of the MM mode is as indicated.

Figure 3 shows room temperature hysteresis loop and FMR results. Graph (a) shows hysteresis loops in induction $4\pi M$ versus static field H format for both perpendicular-to-plane (PTP) and in-plane (IP) fields. Graph (b) shows the 60 GHz in-plane field FMR response in a normalized absorption derivative versus H format. The open circles show the data. The solid line shows Lorentzian derivative fit to the strong data peak only, labeled as the main mode. The much weaker modes at lower H-values with the standing spin wave (SSW) label denote higher order standing spin wave modes. The peak on the high-field side of the main mode is labeled as the surface mode.

Consider first the hysteresis loop data in (a). The loops for both field directions give nominal high field $4\pi M_s$ saturation induction values of 4 kG, close to the reported $4\pi M_s$ value for single layer low loss barium ferrite films.[9] In addition, the overall shapes of the loops confirm the expected perpendicular-to-plane uniaxial anisotropy for the BaM layer. The IP loop saturation field $H_{IP\text{-}sat}$ is 16 kOe or so. This corresponds to the effective uniaxial anisotropy field H_u for the film. An H_u value of 16 kOe matches closely to measured values for single-crystal films and bulk BaM materials.[9,11]

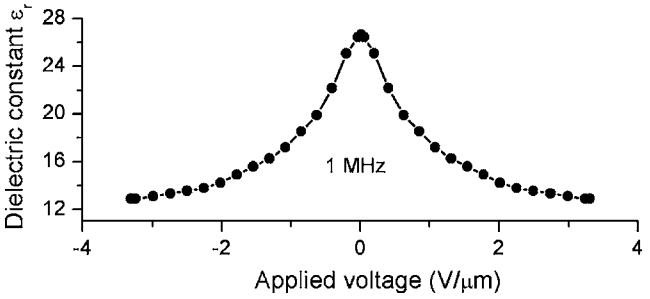

FIG. 4. The BSTO relative dielectric constant ε_r vs applied voltage for the BaM-BSTO layered structure, based on 1 MHz capacitance measurements.

Consider next the FMR results in (b). One sees the main mode sits at about 9.4 kOe. The peak-to-peak linewidth is about 25 Oe. The position is consistent with the H_u and $4\pi M_s$ from the static data in (a). The 25 Oe FMR linewidth is only slightly higher than the reported intrinsic linewidths in bulk single crystals and single layer films.[9,11] These extra losses may be due to the fact that the BaM layer is highly *c*-axis oriented but not really single crystalline. In any event, these results show that one can achieve a low BaM FMR loss even in a layered structure with gold and BSTO layers present. The presence of the weak modes at low field gives additional evidence of film quality.

Figure 4 shows electric response data, through a plot of the BSTO relative dielectric constant ε_r versus the voltage across the gold electrodes as obtained from 1 MHz capacitance measurements. The cusp response and the more than a factor of 2 change in ε_r demonstrates the electric field tunability of the layer. It is to be noted, however, that the nominal ε_r value for conventional 100 nm thick films is about 1200. The substantially lower value seen here likely indicates a fair amount of gold diffusion into the BSTO layer during the 600 °C deposition. Such gold diffusion also affects the operational thickness of the BSTO layer and the corresponding calibration of the capacitance measurement of ε_r.

In summary, dual tunable ferrite-ferroelectric thin film structures with low FMR linewidths have been produced. Future work should focus on (1) demonstrations of the direct tuning of the FMR peak positions with electric fields and response analyses in terms of the hybrid magnetoelectric hybrid modes in the structures, and (2) the use of different electrode materials, such as platinum, to reduce diffusion and enhance the ε_r response.

This work was supported in part by ARO-DARPA Multifunctional Materials Seedling Program under Contract No. W911NF-06-1-0163, MURI Grant No. W911NF-04-1-0247, and the Russian Foundation for Basic Research under Grant No. 05-02-17714. Dr. S. Kohli and Dr. P. McCurdy are acknowledged for the XRD and SEM measurements.

[1] G. Srinivasan, E. T. Rasmussen, J. Gallegos, R. Srinivasan, Y. I. Bokhan, and V. M. Laletin, Phys. Rev. B **64**, 214408 (2001).
[2] V. E. Demidov, B. A. Kalinikos, and P. Edenhofer, J. Appl. Phys. **91**, 10007 (2002).
[3] H. Zheng, J. Wang, S. E. Lofland, Z. Ma, L. Mohaddes-Ardabili, T. Zhao, L. Salamanca-Riba, S. R. Shinde, S. B. Ogale, F. Bai, D. Viehland, Y. Jia, D. G. Schlom, M. Wuttig, A. Roytburg, and R. Ramesh, Science **303**, 661 (2004).
[4] L. C. Sengupta and S. Sengupta, IEEE Trans. Ultrason. Ferroelectr. Freq. Control **44**, 792 (1997).
[5] A. A. Semenov, S. F. Karmanenko, B. A. Kalinikos, G. Srinivasan, A. N. Slavin, and J. V. Mantese, Electron. Lett. **42**, 641 (2006).
[6] A. B. Ustinov, V. S. Tiberkevich, G. Srinivasan, A. N. Slavin, A. A. Semenov, S. F. Karmanenko, B. A. Kalinikos, J. V. Mantese, and R. Ramer, J. Appl. Phys. **100**, 093905 (2006).
[7] R. Heindl, H. Srikanth, S. Witanachchi, P. Mukherjee, T. Weller, A. S. Tatarenko, and G. Srinivasan, J. Appl. Phys. **101**, 09M503 (2007).
[8] S. D. Yoon, C. Vittoria, and S. A. Oliver, J. Appl. Phys. **93**, 4023 (2003).
[9] Y. Song, S. Kalarickal, and C. E. Patton, J. Appl. Phys. **94**, 5103 (2003).
[10] J. Das, B. Griffin, and C. E. Patton, Ninth Intermag Conference, San Diego, California, 8–12 May 2006 (unpublished), Paper No. EU.08.
[11] R. Karim, K. D. McKinstry, J. R. Truedson, and C. E. Patton, IEEE Trans. Magn. **28**, 3225 (1992).